Journal of Affective Disorders 212 (2017) 78–85

Contents lists available at ScienceDirect

Journal of Affective Disorders

journal homepage: www.elsevier.com/locate/jad

Research paper

Alterations of functional connectivity and intrinsic activity within the cingulate cortex of suicidal ideators

Henry W. Chase[a,*], Anna Maria Segreti[a], Timothy A. Keller[b], Vladimir L. Cherkassky[b], Marcel A. Just[b], Lisa A. Pan[a], David A. Brent[a]

[a] Department of Psychiatry, University of Pittsburgh School of Medicine, Pittsburgh, PA, United States
[b] Department of Psychology, Carnegie Mellon University, Pittsburgh, PA, United States

ARTICLE INFO

Keywords:
Default mode network
Suicidal ideation
Resting state fMRI
Functional connectivity
Low frequency oscillations
Diffusion tensor imaging

ABSTRACT

The 'default mode network' (DMN), a collection of brain regions including the posterior cingulate cortex (PCC), shows reliable inter-regional functional connectivity at rest. It has been implicated in rumination and other negative affective states, but its role in suicidal ideation is not well understood. We employed seed based functional connectivity methods to analyze resting state fMRI data in 34 suicidal ideators and 40 healthy control participants. Whole-brain connectivity with dorsal PCC or ventral PCC was broadly intact between the two groups, but while the control participants showed greater coupling between the dorsal anterior cingulate cortex (dACC) and dorsal PCC, compared to the dACC and ventral PCC, this difference was reversed in the ideators. Furthermore, ongoing low frequency BOLD signal in these three regions (dorsal, ventral PCC, dACC) was reduced in the ideators. The structural integrity of the cingulum bundle, as measured using diffusion tensor imaging (DTI), also explained variation in the functional connectivity measures but did not abolish the group differences. Together, these findings provide evidence of abnormalities in the DMN underlying the tendency towards suicidal ideation.

1. Introduction

The posterior cingulate cortex (PCC) – a prominent hub within the default mode network (DMN) - shows robust activation and connectivity during the resting state, and relatively greater activation when individuals are not engaging in stimulus-led cognitive tasks (Greicius et al., 2003; Pfefferbaum et al., 2011). The region is thought to play a role in self-referential processing and forms of reflective, internally directed thought (Johnson et al., 2009), and is of particular relevance for understanding the type of neurocognitive processes which may underlie negative affective states – including rumination, brooding and suicidal ideation - that accompany mood disorders. In addition, its functional interaction with distal regions such as medial regions of the prefrontal cortex (PFC), and regions of the temporal and parietal lobes may play a crucial part in this role.

Although the resting state is psychologically unconstrained (Morcom and Fletcher, 2007), alterations in functional connectivity between brain regions that accompany depressive illness may be observed, due to the relationship between mind wandering and negative mood (Smallwood et al., 2009). However, whilst evidence from case controlled studies of depression using resting state fMRI has been plentiful, a reliable signature of altered DMN connectivity has been somewhat elusive (but see Hamilton et al., 2015; Kaiser et al., 2015). Two factors are likely to have impeded identifying such a signature, regardless whether or not it indeed exists.

First, the marked heterogeneity of mood disorders (e.g. Sullivan et al., 1998) is particularly important in this context. This heterogeneity may be manifest in terms of both state (i.e. current mood state) and trait (i.e. the predisposition toward a particular mood state). The unconstrained nature of the resting state may both afford an opportunity to examine rumination, brooding and other negatively-valenced cognition, but also limits the capacity to manipulate them experimentally. In particular, Berman and colleagues (Berman et al., 2011; see also Hamilton et al., 2011) observed heightened connectivity within the DMN during rest periods in MDD patients compared to controls, particularly those who showed higher levels of rumination. Such associations were not observed during task performance.

Individual differences in rumination and brooding are related to suicidal ideation (Miranda and Nolen-Hoeksema, 2007), and components of impaired problem solving and cognitive inflexibility (e.g. McGirr et al., 2012; Miranda et al., 2013; Whitmer and Banich, 2007; Whitmer and Gotlib, 2012) are relevant to each. There are key

* Correspondence to: Western Psychiatric Institute and Clinic, Loeffler Building, 121 Meyran Avenue, Pittsburgh 15213, PA, United States.
E-mail address: chaseh@upmc.edu (H.W. Chase).

http://dx.doi.org/10.1016/j.jad.2017.01.013
Received 3 October 2016; Received in revised form 27 November 2016; Accepted 14 January 2017
Available online 15 January 2017
0165-0327/

areas of divergence, however, involving the role of impulsivity and entrapment in influencing the onset of suicidal ideation and attempt (Dhingra et al., 2016). Moreover, the morbid aspects of ongoing thought, including the consideration of method and intent in the case of those at risk of suicide, may represent a further aspect of divergence from rumination and brooding. However, to our knowledge, there has been relatively little investigation of resting state neuroimaging in suicidal attempters or ideators (Cao et al., 2015; Fan et al., 2013; Zhang et al., 2016; see Desmyter et al., 2011; Serafini et al., 2016 for reviews). In the present study, we examined connectivity within the DMN within a group of young adults displaying high levels of suicidal ideation and compared them with a cohort of healthy controls.

A second factor that might hinder the identification of an altered DMN signature of negative affective state is the variety of analytical strategies that have been employed to examine functional connectivity. In particular, underspecified seed regions may reduce the reliability of seed-based resting state studies (Cole et al., 2010). Although the PCC is often treated as a single functional entity, recent data-driven modeling approaches have revealed evidence that the region consists of several, distinct regions with particular functions (Bzdok et al., 2015). Leech and colleagues (Leech et al., 2011) identified dorsal and ventral subregions of the PCC, which showed differential interactions with cognitive control networks (CCN e.g. the dorsal anterior cingulate cortex (dACC) and dorsolateral PFC) and the DMN itself. The ventral region was more closely coupled to the DMN but less to the CCN during a simple (0-back) task. However, this pattern changed during the more difficult 2-back task, with coupling with the DMN falling and coupling increasing with the CCN. By contrast, the dorsal PCC region showed the opposite pattern – relatively reduced coupling with the DMN and relatively enhanced coupling with the CCN during the simple task, but increasing and decreasing connectivity respectively during the more difficult condition. The authors argued that the interaction of the two regions is required for the orchestration of large scale networks during tasks of varying complexity. Here, we examined the connectivity of dorsal and ventral PCC seeds separately, and also examined their difference maps, hypothesizing that the ideators would show an altered pattern of connectivity within the DMN.

More recent statistical considerations of resting state functional connectivity have highlighted ambiguities with the commonly employed Pearson's R statistic (Cole et al., 2016) and, by consequence, related methods of statistical association. In particular, this measure of connectivity is a function of the covariance between regions – which is assumed to reflect the capacity for information transfer between regions - but also their variance. It is therefore possible that two groups may show similar covariance between regions, but differ with respect to irrelevant variance: a sole reliance on correlation would be misleading in this context. A related possibility is that the intrinsic activity of a given region might be altered within particular frequency components of the signal, which may provide some indirect influence on raw variance estimates. More importantly, it may reflect alterations in ongoing neural processing in that region that may have ramifications for functional connectivity (Baria et al., 2013). We therefore also examined intrinsic low-frequency activity – given that this dominates rsfMRI BOLD signal - of the key DMN nodes, in order to provide further characterization of DMN activity.

Finally, following van den Heuvel and colleagues (van den Heuvel et al., 2008), we examined the extent to which alterations in structural connectivity, as measured using diffusion tensor imaging (DTI), were responsible for any functional changes observed, particularly focusing on the cingulum bundle.

2. Methods

2.1. Participants

79 total adult participants were assessed, five participants (2SI, 3HC) were excluded due to excessive movement (total movement > 3 mm), leaving a final sample of 74. In addition, three of the control participants did not have DTI data. Participants were age 18–35 and consisted of 40 healthy controls (HC) with no personal or family history of psychiatric disorder or suicide attempt; and 34 patients with current suicidal ideation (SI) which was determined at recruitment during the screening process, and was confirmed at the study visit with the Suicidal Ideation Questionnaire (SIQ: cut off score > 20) and the Columbia Suicide Severity Rating Scale (C-SSRS: cut off score 4 or 5 for the first two questions). About half of the SI population had a history of previous suicide attempt (n=18). All healthy controls needed to have scored below clinical cutoffs on all self-report measures in addition to having no current or past suicidal ideation and behavior.

Participants were screened by the psychiatrist with respect to safety to participate in an fMRI study, ability to commit to a safety plan and not engage in self-harm while participating in the study. Participants were also screened by the psychiatrist with respect to present or past psychotropic medication, mental health treatment, and suicidal behavior, with the latter using the Columbia Suicide History Form. Current psychiatric symptomatology and suicidal ideation/behavior were assessed by the interview-rated suicidal ideation and behavior, using the C-SSRS, self-reported depression and anxiety using the PHQ-9 and State-Trait Anxiety Scale, suicidal ideation using the SIQ, and both narrow and broad band psychopathology using the Adult Self-Report. Patient diagnoses and medication status were obtained via medical records, and symptom inventories describe current symptoms (see Table 1).

The sample was recruited from the UPMC Clinical and Translational Science Institute Registry, UPMC outpatient clinical services, advertisements, and existing studies within our lab. Exclusion criteria included neurological disorders, head injury, Verbal Subtest of the Wechsler Intelligence Test (Wechsler, 1999) score < 80, use of sedative medication, drug or alcohol disorder or positive urine drug screen, pregnancy, MRI ineligibility, and psychosis. Any SI with suicide attempt causing neurological damage or long term physiologic effects was excluded.

Ethical approval for the study was obtained from both the University of Pittsburgh and the Carnegie Mellon University Institutional Review Boards, and informed consent was obtained for all participants.

2.2. MRI acquisition sequences

Neuroimaging data were collected using a 3.0 T Siemens Magnetom Verio MRI scanner in the Scientific Imaging and Brain Research Center at Carnegie Mellon University with a 32-channel Siemens receive coil. BOLD Resting State images were acquired with a 5 min Siemens gradient echo planar imaging (ep2d-bold) sequence with eyes open (300 successive brain volumes) covering 20 axial slices (5.0 mm thick; repetition time: 1000 ms; echo time: 25 ms; FOV: 200 mm; flip angle: 60°; matrix=64×64; GRAPPA acceleration (iPAT) factor: 2). Field map images were also acquired (repetition time: 572 ms; echo time: 5.00 ms; echo time2: 7.46 ms; FOV: 230 mm; flip angle: 70°; matrix: 96×96).

Structural three dimensional axial magnetization prepared rapid acquisition gradient echo (MPRAGE) images were acquired (repetition time: 1700 ms; echo time: 2.48 ms; inversion time: 900 ms; flip angle: 9°; FOV: 256 mm; matrix: 256×256). Diffusion-weighted structural images were acquired using the multi-band sequences (version R011 for Syngo VB17A) with the monopolar cmrr_mbep2d_diff sequence provided by the University of Minnesota Center for Magnetic Resonance Research (https://www.cmrr.umn.edu/multiband/) in 54 slices (matrix: 96×96, FOV: 230 mm; 2.4-mm isotropic voxels; TR=2264 ms; TE=74.8 ms; multi-band acceleration factor: 3; number of diffusion encoded directions: 30; diffusion b-value: 1000s/mm^2, number of non-diffusion encoded images: 4; bandwidth: 1860 Hz/

Table 1
Demographic information and clinical variables: SI: suicide ideators, HC: healthy controls; WASI (IQ): Wechsler Abbreviated Scale of Intelligence, PHQ: Patient Health Questionnaire; SIQ: Suicidal Ideation Questionnaire; CTQ: Childhood Trauma Questionnaire; STAI-T: Spielberger State Trait Anxiety Inventory - Trait; ASR: Adult Self Report. Of the 34 patients, 30 were diagnosed with major depressive disorder (MDD), 21 were diagnosed with general anxiety disorder (GAD); 6 with Bipolar I or II, 4 with borderline personality disorder, 2 with post-traumatic stress disorder (PTSD), and one each with cerebral folate deficiency, post-partum depression, anorexia, Tourette's disorder, obsessive compulsive disorder, Asperger's disorder, and Attention Deficit Disorder. One patient was trans-gender (female to male). All patients were medicated, typically with antidepressants and/or mood stabilizers.

		SI (n=34)	HC (n=40)	Statistic (T test unless stated)	p value
Gender	Male	7	17		
	Female	27	23	X^2=4.03	0.045
Mean age (years)		24.41 (S.D.: 5.51)	22.15 (S.D.: 2.88)	2.13	0.038
WASI (IQ)		116.97(S.D.: 14.57)	121.08 (S.D.: 9.48)	−1.41	0.15
PHQ		12.15 (S.D.: 6.32)	0.5 (S.D.: 1.18)	10.59	< 0.001
SIQ		57.26 (S.D.: 31.63)	2.28(S.D.: 4.77)	10.041	< 0.001
CTQ		50.85 (S.D.: 19.38)	30.73 (S.D.: 7.44)	5.71	< 0.001
STAI-T		48.26 (S.D.: 5.29)	46.50 (S.D.: 3.50)	1.66	0.10
ASR					
Subscales:					
1. Anxious/Depressed		21.35 (S.D.: 7.13)	4.48 (S.D.: 4.11)	12.18	< 0.001
2. Withdrawn		6.65(S.D.: 3.25)	1.45 (S.D.: 1.50)	8.59	< 0.001
3. Somatic complaints		7.06(S.D.: 4.61)	1.30(S.D.: 2.11)	6.71	< 0.001
4. Thought problems		5.74(S.D.: 2.84)	1.25 (S.D.: 1.46)	8.31	< 0.001
5. Attention problems		13.59 (S.D.: 5.97)	4.18 (S.D.: 3.45)	8.12	< 0.001
6. Aggressive behavior		9.65(S.D.: 4.83)	2.45 (S.D.: 2.45)	7.87	< 0.001
7. Rule breaking		4.29 (S.D.: 3.30)	1.68(S.D.: 1.70)	4.18	< 0.001
8. Intrusive		2.00 (S.D.: 1.84)	1.83 (S.D.: 2.04)	0.39	0.70
9. Internalizing problems		35.06 (S.D.: 11.11)	7.23 (S.D.: 6.24)	12.98	< 0.001
10. Externalizing problems		15.94 (S.D.: 8.46)	5.95 (S.D.: 4.73)	6.12	< 0.001
11. Total problems		86.50 (S.D.: 25.18)	24.63(S.D.: 17.13)	12.51	< 0.001

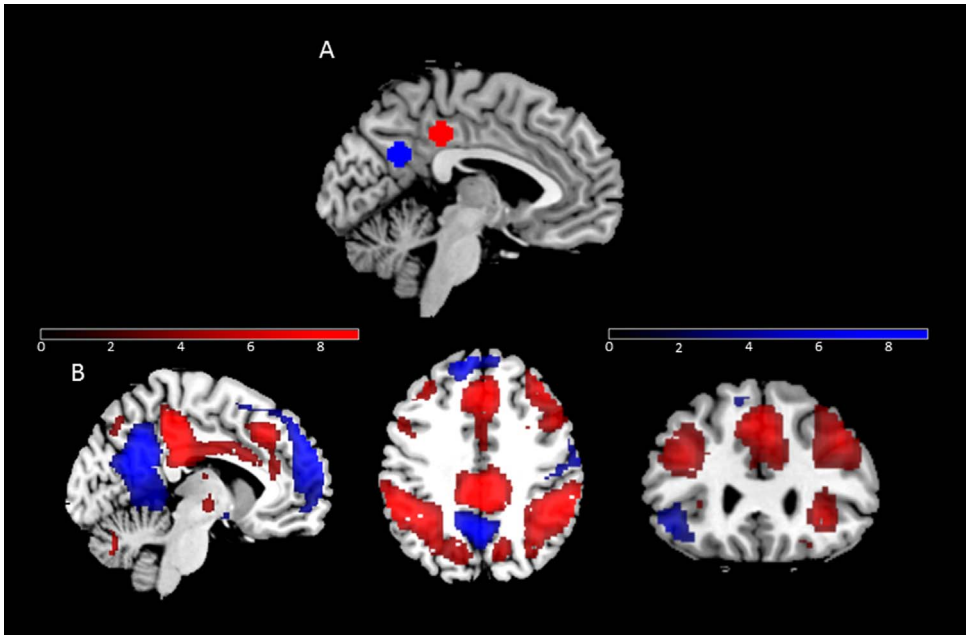

Fig. 1. A) Default mode network seeds: dPCC (red), vPCC (blue). B) Low frequency BOLD activity for the two posterior cingulate seed regions (red: dorsal > ventral; blue: ventral > dorsal). Thresholded at $p < 0.001$ for display purposes. Scale reflects T statistics. (For interpretation of the references to color in this figure legend, the reader is referred to the web version of this article).

Pixel; partial Fourier factor: 6/8). This entire DTI sequence was acquired twice for each participant with opposite phase encoding directions (anterior to posterior (AP) and posterior to anterior (PA)) so that geometric distortions and eddy currents could be corrected. Diffusion-weighted, field-mapping, and functional images were all collected as oblique-axial scans aligned with the Anterior Commissure-Posterior Commissure (AC-PC) line at midline.

2.3. Functional imaging preprocessing and analysis

Images were preprocessed using standard SPM8 tools. These steps included slice timing correction, correction for motion (realignment) and unwarping using a field map, coregistration of the unwarped image to the participant's structural image. Images were then normalized using the 'unified segmentation' approach, including segmentation of the structural image and registration into Montreal Neurological Institute (MNI) space (ICBM template), and then registration of functional image to MNI space based on the parameters of the structural registration. Finally, normalized images were smoothed using a 6 mm FWHM Gaussian kernel.

Following preprocessing, first (participant) level analysis of resting state images involved a general linear model-based method implemented in SPM8 (see also Chase et al., 2013). Specifically, timeseries were extracted for each seed region (see below), nuisance corrected and

filtered at two frequencies (Low 0.01–0.08 Hz; Mid 0.08–0.15 Hz) using custom MATLAB scripts. Nuisance correction involved estimation of the global signal, 6 motion parameters, and five components obtained from a CompCor-like algorithm (Behzadi et al., 2007). With respect to the latter, data were extracted from a white matter and cerebro-spinal fluid (CSF) mask, as well as timeseries with a high standard deviation, for each participant, and combined into a single data matrix. Principal Components Analysis (PCA) was performed on the resulting data, and the five components representing the majority of variance within the data array were included as nuisance regressors. The processed (nuisance corrected/filtered) mid and low frequency timeseries from the seed region were fitted to each voxel in the brain using a GLM implemented in SPM8, in a model which also included all twelve nuisance regressors and a 143 s high pass filter. Correction for autoregressive noise (AR(1)) was also performed within the GLM model. The two 8 mm-radius PCC seed regions were defined on the basis of Leech et al. (2011): see Fig. 1A), a dorsal PCC (MNI: x=0, y=−34, z=40) and a ventral PCC (MNI: x=0, y=−58, z=28) seed, although we set the x coordinates to zero rather than small non-zero values.

2.4. Timeseries analysis

A number of follow up analyses were performed on the raw, extracted timeseries within the regions of interest (ROI) to characterize the underlying neurophysiological differences further. First, timeseries were extracted from the three ROIs – dPCC, vPCC and the dACC – for each participant. The dACC was represented by an independently defined ROI of the region (region 3 in Beckmann et al., 2009), from a parcellation which defined the extent of each sub-region in y and z dimension. An ROI was created by extending the region in the x dimension. The extracted timeseries were then subject to nuisance regression using the same CompCor, global signal and motion variables as used in the whole brain analysis described above, as well as a linear trend across the timeseries. In contrast to this analysis however, the residual timeseries were not filtered, in order to demonstrate the generality of the findings across different processing methods. Functional connectivity was examined by computing Pearson's correlation coefficient between the corrected timeseries for each individual/ROI, and then Z transforming the resulting R statistic. A metric of low frequency (LF) BOLD signal was computed using the Welch transformation (Baria et al., 2013; Welch, 1967), and computing the ratio of power between 0 and 0.08 Hz activity (i.e. low frequency) and power between 0.08 and 0.25 Hz (i.e. high/mid frequencies). The resulting statistic was then log transformed.

2.5. Diffusion tensor imaging (DTI)

Preprocessing of the diffusion tensor images (DTI) made use of tools from FSL v.5.0.8 (http://fsl.fmrib.ox.ac.uk/fsl/fslwiki/) (Smith et al., 2004), and code written in-house for motion correction of diffusion data (Jung et al., 2013; Jung, 2010) running under MATLAB®, v. R2011a (www.mathworks.com/products/matlab). Brain-only masks of images at each stage of the following procedures were extracted using the FSL's "bet2." Estimation and correction of geometric distortion was carried out for each session (pre-training and post-training) using the eight non-diffusion-weighted images (b-value =0), four collected with each phase encoding direction (A > P, P > A) (Andersson et al., 2003). FSL's "topup" tool was first used to estimate a warp-field and the data were subsequently resliced and the two diffusion runs averaged using the "applytopup" tool. FSL's "eddy" tool was then used to simultaneously model the eddy current effects and head motion effects in the run-averaged data using default values for all parameters (i.e., a quadratic spatial model, no spatial filtering, and five iterations of the non-linear estimation).

Additional pre-processing involved generation of an estimated diffusion tensor image for each corrected diffusion tensor image on the basis of average signal intensities across the corrected un-weighted (b-value =0) images (Jung et al., 2013). Given the acquisition parameters of each image the estimated signal for each voxel in each diffusion direction can then simply be derived from the Bloch-Torrey equation (Torrey, 1956), resulting in a "simulated" diffusion-weighted image that is perfectly co-registered to the mean of the corrected un-weighted images. We then used each simulated image as the target for a 12-parameter affine co-registration with the corresponding corrected DTI. This estimation and reslicing was carried out with FSL's "mcflirt" program, using a correlation ratio cost function. Finally, each of the affine transformation matrices computed above were combined, and a single reslicing of the original data was carried out with FSL's "applywarp" and the direction of the diffusion vectors were rotated on the basis of this combined transformation prior to fitting a weighted-least squared diffusion tensor model with FSL's "dtifit."

We used FSL's "fnirt" tool with default parameters for fractional anisotropy (FA) to FA non-linear co-registration, to estimate the warping from each participant's FA map to the FMRIB_FA_1mm template included in FSL. This nonlinear warping was applied to each of the scalar DTI measure maps for each participant and session. We then extracted the scalar diffusion measures for each participant from each of the atlas-defined tracts in the Illinois Institute of Technology (IIT) Human Brain Atlas (Varentsova et al., 2014).

Inference was restricted to the cingulum bundle following (van den Heuvel et al., 2008), focusing on the relationship between DTI measures (a left/right cingulum combined score) and our measures of functional connectivity: FA, radial diffusivity (RD) and axial diffusivity (AD). As well as attempting to identify a relationship between DTI and functional connectivity, we also sought to establish the extent to which effects of group on functional connectivity measures might be independent of any differences in DTI measures.

2.6. Analytical strategy

For the functional images, whole brain analyses were focused on the low frequency timeseries. Connectivity maps for the dorsal and ventral seed, and dorsal minus ventral seed were analyzed at the group level: both the main effect of the seed and group differences (ideators versus controls) were examined using *t*-tests. An additional set of analyses were performed to contrast attempters and non-attempters at the whole brain. Motion (maximum translation in any of the x, y or z dimensions), age, and gender were included in the model as covariates of no interest. Significance was assigned on the basis of a family wise error-corrected (FWE) cluster threshold of $p < 0.05$ based on Gaussian random field theory, using a cluster forming threshold of $p < 0.001$ (Flandin and Friston, 2016).

In addition, two further dependent measures were derived from the timeseries analysis: functional connectivity measures and low frequency BOLD signal. These measures were then submitted to repeated-measures analysis of variance (ANOVA) to establish the effects of group, and interactions by region. In addition, correlational analyses were performed to explore the effects of individual differences in DTI measures of the cingulate bundle (see above), and in questionnaire measures, and their inter-relationships with low frequency BOLD and functional connectivity. These analyses were performed across all participants, and within each group separately. For completeness, all findings that reached or approached a significance level of $p < 0.05$ were reported.

3. Results

3.1. Main effects

Low frequency BOLD activity within both dorsal and ventral PCC seeds showed robust coupling across participants with other regions of

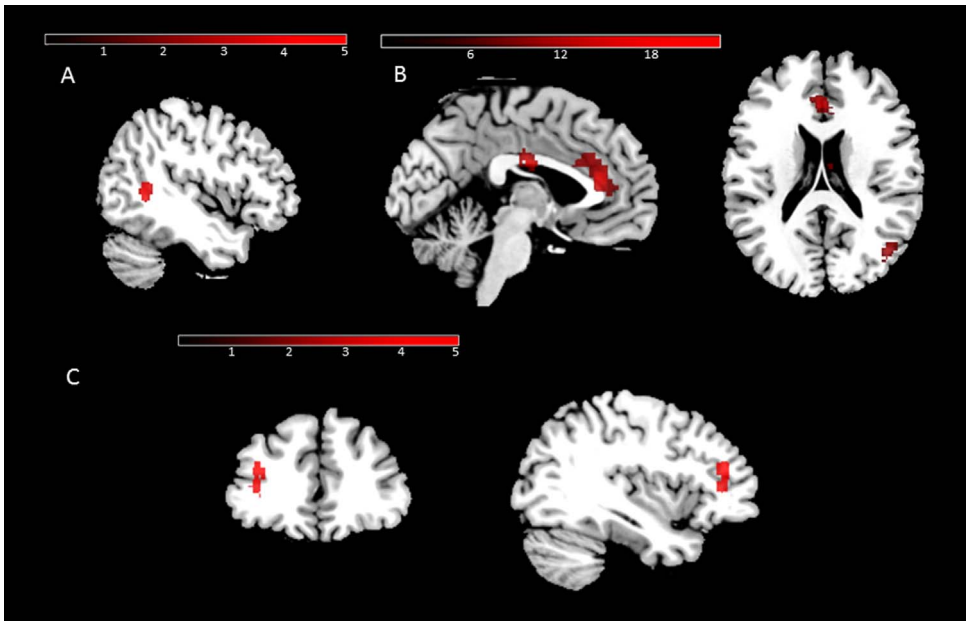

Fig. 2. A) Figure showing the group differences in connectivity between the dPCC and the left temporal lobe. Scale reflects T statistics. B) Figure highlighting the dACC cluster which demonstrates greater dPCC compared to vPCC connectivity in controls compared to ideators. Scale reflects F statistics, as the contrast shows the main effect of group for completeness. C) Figure displaying the contrast of attempters and non-attempters with the dPCC seed, which yielded a group difference in the left inferior frontal gyrus. Scale reflects T statistics. In all cases, the contrasts were thresholded at $p < 0.001$ uncorrected for display purposes. (For interpretation of the references to color in this figure legend, the reader is referred to the web version of this article).

the DMN, including the medial PFC, inferior parietal cortex, superior temporal gyrus, thalamus, and the medial temporal lobe (hippocampus). Comparison of the dorsal and ventral seed revealed greater interactions of the dorsal region with the dorsal anterior and mid-cingulate, anterior insula, dorsolateral PFC, parietal cortex, thalamus and striatum (anterior caudate). The ventral PCC showed greater connectivity with a rostral region of the medial prefrontal cortex, the left ventrolateral PFC, retrosplenial cortex, medial temporal lobe, occipitotemporal regions such as the fusiform/parahippocampal gyrus (see Fig. 1B). Similar patterns of findings were seen with mid frequency maps, but these were somewhat weaker and not pursued further statistically.

3.2. Group differences in connectivity

Ideators showed significantly more positive between the dorsal PCC and the left middle temporal gyrus (xyz co-ordinates: −42 −52 6; T=4.68, k=171, p_FWE=0.025: Fig. 2A). This was caused by a reduced anticorrelation between the dorsal PCC and this region in the ideators compared to controls. No regions of significantly enhanced dorsal PCC connectivity were observed in controls compared to ideators, nor were any significant differences found with the ventral PCC seed.

A group difference in the dACC emerged when comparing the dorsal/ventral PCC difference maps (xyz coordinates: 0 32 16; T=4.23, k=181, p_FWE=0.021; see Fig. 2B). This finding was corroborated using the extracted timeseries data: an effect of group was also seen on differential dPCC-dACC/vPCC-dACC functional cconnectivity (T(72) =2.78, p=0.007: Fig. 3B). Individual differences in motion had a marginally significant effect if also included as a predictor (T=1.98, p=0.051), but correcting for this variance did not affect the significance of the effect of group (T=2.92, p=0.005).

3.3. Intrinsic activity within cingulate cortex

Next, we sought to examine whether intrinsic activity within each of the three regions of interest was also altered in the ideation group. A main effect of region was observed ($F(2, 144)=111.27$, $p < 0.001$), and a main effect of group ($F(1, 72)=5.58$, p=0.021: Fig. 3A), but no interaction between group and region ($F < 1$). The main effect of group reflected a reduction in relatively low frequency power in the ideators, while the regions differed markedly in relative low frequency activity (vPCC > dPCC > dACC: p's all < 0.001).

In general, the vPCC/dACC and dPCC/dACC connectivity was positively related to low frequency (LF) BOLD in these ROIs across both groups (F's~=5–17), such that individuals with greater LF BOLD showed greater connectivity values. However, the relationship between the dPCC-dACC connectivity and dPCC LF BOLD was altered between the groups (group by LF BOLD interaction: $F(1,70)=4.71$, p=0.033), such that the correlation was greater in the patient (r=0.50, p=0.003) than the control group (r=−0.014, p=0.93).

3.4. Diffusion Tensor Imaging (DTI) measures

Cingulate bundle FA tended to differ between the groups ($T(69) =1.71$, p=0.091) but was not related to functional connectivity (FC) measures (all p's > 0.3) (Table 2). Neither the cingulate AD nor RD metric differed between the groups (T's < 1), and neither were related to the pairwise connectivity measures (p's > 0.1). However, RD was related to the dPCC-dACC/vPCC-dACC FC difference (r=−0.24, p=0.04), which remained significant if motion and gender were included in a regression model (T=−2.16, p=0.034). If group was also included, the effect of group remained significant (T=3.036, p=0.003), but cingulate RD was reduced to trend level (T=−1.95, p=0.056). Finally, across both groups, a relationship was observed between cingulate FA and dPCC LF BOLD (r=0.29, p=0.015), and at trend level with the dACC (r=0.23, p=0.059) but not the vPCC (p > 0.4). Neither AD nor RD were related to LF BOLD across all subjects (p's > 0.1). However, RD and LF BOLD relationships showed a marked difference between groups, which was not seen for the AD or FA. In the SI group, RD showed a negative relationship with dPCC LF BOLD (r=−0.48, p=0.004), but a non-significant positive relationship in controls (r=0.12, p=0.48), while RD showed a positive relationship with vPCC LF BOLD in controls (r=0.39, p=0.017) but a non-significant negative relationship in the SI group (r=−0.21, p=0.24).

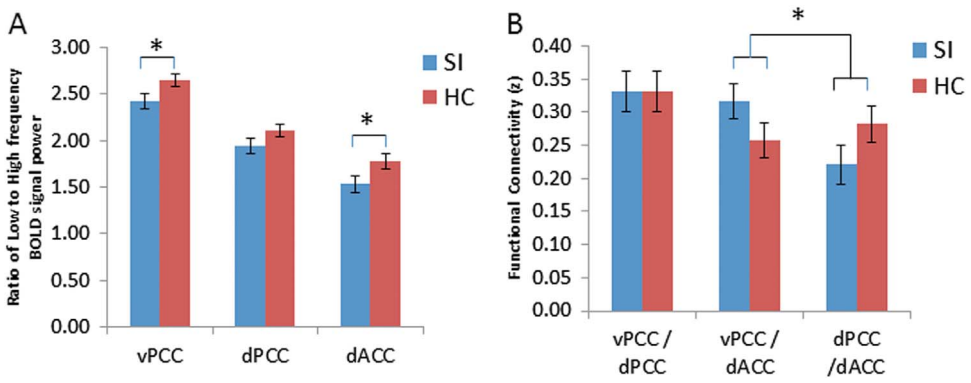

Fig. 3. Low frequency BOLD activity (A) and inter-region functional connectivity (B) for the three regions of interest (ventral PCC, dorsal PCC, dorsal ACC) generated from the timeseries analysis. For the low frequency BOLD (A), a main effect of group was observed, but the significant ($p < 0.05$) differences are marked with a star. For the functional connectivity (B), the significant interaction term is marked with a star. Error bars reflect standard error of the mean.

Table 2
Group comparison of DTI data, describing Z scores for healthy controls (HC) and suicidal ideators (SI), their comparison and 95% confidence interval (CI) around the mean difference.

	SI (mean/ SD)	HC (mean/ SD)	T-test (p value)	95% CI (low, mean, high)
Cingulate FA Z	−0.21 (0.17)	0.19 (0.16)	T=-1.71 (p=0.091)	−0.87/−0.40/ 0.066
Cingulate AD Z	0.073 (0.19)	−0.067 (0.15)	T < 1	−0.34/0.14/ 0.62
Cingulate RD Z	−0.11 (0.17)	0.12 (0.16)	T < 1	−0.25/0.23/ 0.70

3.5. Attempters versus non-attempters

We conducted a series of planned comparisons between the attempters and non-attempters. Of these analyses, the dPCC/vPPC and vPCC seed analyses did not yield any significant findings. However, a marginal difference was seen in the left inferior frontal gyrus when using the dPCC seed, with attempters showing more positive connectivity than non-attempters (without covariates: xyz co-ordinates=−40, 32, 10; peak T=4.16,k=139, cluster p_FWE=0.039; with covariates: xyz=−38, 40, 20; peak T=4.82,k=120, p_FWE=0.054: Fig. 2C).

3.6. Questionnaires

We examined the association between the primary neurophysiological measures of interest and the following questionnaire variables: SIQ, ASQ thought problems and internalizing problems, and number of attempts. Across all participants, marginal relationships were seen between the dPCC-dACC/vPCC-dACC FC difference with internalizing problems (rho=−0.27, p=0.022), SIQ (rho=−0.23, p=0.050) and attempts (rho=−0.23, p=0.053) but these were largely driven by group. In the ideators alone, there were marginal relationships between SIQ and LF BOLD in the dPCC (rho=0.33, p=0.058) and FA and thought problems (rho=−0.32, p=0.066); while in the controls alone, there was a relationship between thought problems and vPCC LF BOLD (rho=0.40, p=0.011).

4. Discussion

In the present study, we have identified altered patterns of functional connectivity in the cingulate cortex in suicidal ideators, with the relative functional connectivity between the dorsal PCC and dorsal ACC, and the ventral PCC and dorsal ACC being altered in ideators compared to controls. This provides further evidence for disrupted connectivity within the default mode network (DMN) accompanying mood disorders (Hamilton et al., 2015) and rumination (Berman et al., 2011; Hamilton et al., 2011; Lois and Wessa, 2016), as well as further support for growing evidence for functional abnormalities within the cingulate cortex associated with suicidal behavior (van Heeringen et al., 2014). In addition, although the connectivity maps of attempter and non-attempter subgroups were largely similar, a marginally significant difference was seen in the left inferior frontal gyrus between attempters and non-attempters, when comparing the connectivity of the dorsal PCC seed. This latter observation may relate to the role of the inferior frontal gyrus in the orchestration of large scale (DMN/CCN) networks (Hamilton et al., 2011).

We focused on two separate dorsal and ventral PCC seeds, following prior work suggesting relative independence of these regions (Leech et al., 2011). The comparison of the two seeds revealed preferential connectivity with cognitive control regions (dPCC) and core DMN regions (vPCC). The implication of the dACC in the relative connectivity of these two nodes of the PCC may reflect a capacity of the region to orchestrate the activity and connectivity of each. Alternatively, given that the BOLD signal in a particular region is more likely to reflect synaptic input to the region (Logothetis and Wandell, 2004), the difference may reflect the output of interactions within PCC subregions themselves. Regardless of its causal role, the identification of the dACC accords with previous evidence from rumination (Kuhn et al., 2012), negative mood induction (Berman et al., 2014; Harrison et al., 2008) and stimuli related to suicidal activity (Reisch et al., 2010).

We have remained mindful of possible features of our statistical models that may influence our results, and the comparison between two seeds would have diminished the impact of relatively non-specific and irrelevant factors such as the influence of global fluctuations, or variation in signal to noise ratio (SNR). It may also have corrected for irrelevant differences in the functional architecture of the DMN that may contribute additional variance, or irrelevant state related effects. Importantly, we also observed altered intrinsic activity within the ROIs themselves, with the ideators showing relatively reduced low frequency (LF) BOLD activity compared to controls. The statistical association we observed between LF BOLD and functional connectivity confirms the intimate relationship between the two (Baria et al., 2013). At present, a causal interpretation is not possible, so we argue that the joint observation of altered functional connectivity and altered intrinsic LF BOLD represent an emergent property of the DMN in ideators.

In addition, DTI measures were associated with functional connectivity and LF BOLD, suggesting that this altered, emergent DMN state may be driven, in part, by the integrity of the cingulum bundle. Although structural connectivity of the cingulum bundle was marginally associated with group (at least FA), a multiple regression analysis suggested that the influence of structural abnormalities and group were broadly statistically distinct. Indeed, it was RD, and not FA, that was most closely related to altered functional connectivity. Although our findings do not parallel those of van den Heuvel et al. (2008), that RD

can be an effective predictor of functional connectivity has been reported previously (Lowe et al., 2014). Lowe et al. argued that RD was reflective of a number of different aspects of white matter integrity, and was thus well positioned to mirror altered functional integration.

Nevertheless, the relationships between DTI and functional measures were relatively weak. The presence of stronger moderated relationships between structure (RD) and intrinsic activity (dPCC/vPCC LF BOLD), and also intrinsic activity (dPCC LF BOLD) and dPCC/dACC connectivity, collectively suggest that abnormal connectivity in the DMN of ideators is not simply a function of a structural deficit, nor reduced intrinsic activity. Rather, these alterations in DMN may reflect an emergent alteration of neural processing, and perhaps also psychological state such as the attentional focus of the individual (Whitmer and Gotlib, 2013). There is some precedent for such an interpretation: Baria and colleagues observed that the relationship between structural connectivity and LF BOLD changed across different cognitive (attentional) states (Baria et al., 2013). The present study relies on a between-subject comparison, rather than a within-subjects comparison however, and thus the inference that attention might be relevant might be strengthened via the investigation of cognitive manipulations.

Finally, connectivity with the dorsal PCC seed and the left temporal lobe was altered in the ideators compared to the controls. We note that a comprehensive study of DMN connectivity identified interactions between the DMN and different sectors of the temporal lobe as being related to aspects of ongoing cognition during the resting state (Smallwood et al., 2016). Further investigation of this phenomenon may therefore involve more detailed measurement of cognitive and affective state during the resting state scan.

4.1. Limitations

Typical limitations of rsfMRI studies apply in the present context. These include the potentially confounding influence of motion and global signal (Murphy et al., 2013). We found no statistical evidence that these were relevant in the present context – the key PCC/dACC connectivity and LF BOLD metrics were very similar whether global signal was corrected for or not, and significance was unaffected by covarying for individual differences in motion. The groups were also somewhat confounded by age and gender, but, likewise, no influence of age or gender were identified when these variable were included as covariates. The acquisition sequence was quite short at 5 min, and a longer sequence may provide some benefits in terms of measurement reliability (Birn et al., 2013).

Another limitation was our inability to identify a key feature of the population characteristics that might provide a crucial influence on the pattern of findings. The sample was relatively heterogeneous in terms of its clinical history and presentation, which opens the possibility that a variety of personality or trait-like variables may influence the pattern of findings. Our attempts to identify these using questionnaire measures revealed only marginal/uncorrected relationships, which were largely related to group membership. This limitation opens a variety of empirical possibilities, which may involve examining the same phenomena with more tightly controlled psychiatric control groups.

A final limitation is one inherent to rsfMRI, namely the uncontrolled nature of cognition. This might be partly remediated using self-report. However, it is intriguing that the cingulate regions identified in the present study are similar to those identified using task-based fMRI (van Heeringen et al., 2014), and may be involved in economic valuation (Dombrovski et al., 2013; Vanyukov et al., 2016). In this light, rsfMRI may provide a compatible line of evidence: the relationship between task- and resting-state fMRI may be extended using other connectivity techniques which may be used to model both states in the same framework (e.g. Piray et al., 2015).

4.2. Summary

Together, our findings provide evidence of abnormalities in resting state functional connectivity in suicide ideators (SI) within the DMN. In particular, we found differential relationships between the dACC with the dorsal and ventral PCC between SI and healthy controls, as well as reduced low frequency BOLD in all three regions in the SI group. It provides one of the first examinations of resting state connectivity in suicidal ideators. Furthermore, our findings highlight the impact of individual differences in the structural integrity of the cingulum bundle, and also differences in intrinsic activity within the DMN. Further characterization of these neurophysiological abnormalities will provide useful constrains to understanding the neural basis of suicidal ideation, and may provide targets for rational interventions on affected circuitry.

References

Andersson, J.L., Skare, S., Ashburner, J., 2003. How to correct susceptibility distortions in spin-echo echo-planar images: application to diffusion tensor imaging. Neuroimage 20, 870–888.

Baria, A.T., Mansour, A., Huang, L., Baliki, M.N., Cecchi, G.A., Mesulam, M.M., Apkarian, A.V., 2013. Linking human brain local activity fluctuations to structural and functional network architectures. Neuroimage 73, 144–155.

Beckmann, M., Johansen-Berg, H., Rushworth, M.F., 2009. Connectivity-based parcellation of human cingulate cortex and its relation to functional specialization. J. Neurosci. 29, 1175–1190.

Behzadi, Y., Restom, K., Liau, J., Liu, T.T., 2007. A component based noise correction method (CompCor) for BOLD and perfusion based fMRI. Neuroimage 37, 90–101.

Berman, M.G., Peltier, S., Nee, D.E., Kross, E., Deldin, P.J., Jonides, J., 2011. Depression, rumination and the default network. Soc. Cogn. Affect. Neurosci. 6, 548–555.

Berman, M.G., Misic, B., Buschkuehl, M., Kross, E., Deldin, P.J., Peltier, S., Churchill, N.W., Jaeggi, S.M., Vakorin, V., McIntosh, A.R., Jonides, J., 2014. Does resting-state connectivity reflect depressive rumination? A tale of two analyses. Neuroimage 103, 267–279.

Birn, R.M., Molloy, E.K., Patriat, R., Parker, T., Meier, T.B., Kirk, G.R., Nair, V.A., Meyerand, M.E., Prabhakaran, V., 2013. The effect of scan length on the reliability of resting-state fMRI connectivity estimates. Neuroimage 83, 550–558.

Bzdok, D., Heeger, A., Langner, R., Laird, A.R., Fox, P.T., Palomero-Gallagher, N., Vogt, B.A., Zilles, K., Eickhoff, S.B., 2015. Subspecialization in the human posterior medial cortex. Neuroimage 106, 55–71.

Cao, J., Chen, J.M., Kuang, L., Ai, M., Fang, W.D., Gan, Y., Wang, W., Chen, X.R., Xu, X.M., Wang, H.G., Lv, Z., 2015. Abnormal regional homogeneity in young adult suicide attempters with no diagnosable psychiatric disorder: a resting state functional magnetic imaging study. Psychiatry Res. 231, 95–102.

Chase, H.W., Moses-Kolko, E.L., Zevallos, C., Wisner, K.L., Phillips, M.L., 2013. Disrupted posterior cingulate-amygdala connectivity in postpartum depressed women as measured with resting BOLD fMRI. Soc. Cogn. Affect. Neurosci..

Cole, D.M., Smith, S.M., Beckmann, C.F., 2010. Advances and pitfalls in the analysis and interpretation of resting-state FMRI data. Front. Syst. Neurosci. 4, 8.

Cole, M.W., Yang, G.J., Murray, J.D., Repovs, G., Anticevic, A., 2016. Functional connectivity change as shared signal dynamics. J. Neurosci. Methods 259, 22–39.

Desmyter, S., van Heeringen, C., Audenaert, K., 2011. Structural and functional neuroimaging studies of the suicidal brain. Prog. Neuro-Psychopharmacol. Biol. Psychiatry 35, 796–808.

Dhingra, K., Boduszek, D., O'Connor, R.C., 2016. A structural test of the integrated motivational-volitional model of suicidal behaviour. Psychiatry Res. 239, 169–178.

Dombrovski, A.Y., Szanto, K., Clark, L., Reynolds, C.F., Siegle, G.J., 2013. Reward signals, attempted suicide, and impulsivity in late-life depression. JAMA Psychiatry.

Fan, T., Wu, X., Yao, L., Dong, J., 2013. Abnormal baseline brain activity in suicidal and non-suicidal patients with major depressive disorder. Neurosci. Lett. 534, 35–40.

Flandin, G., Friston, K.J., 2016. Analysis of family-wise error rates in statistical parametric mapping using random field theory. arXiv.

Greicius, M.D., Krasnow, B., Reiss, A.L., Menon, V., 2003. Functional connectivity in the resting brain: a network analysis of the default mode hypothesis. Proc. Natl. Acad. Sci. USA 100, 253–258.

Hamilton, J.P., Farmer, M., Fogelman, P., Gotlib, I.H., 2015. Depressive rumination, the default-mode network, and the dark matter of clinical neuroscience. Biol. Psychiatry 78, 224–230.

Hamilton, J.P., Furman, D.J., Chang, C., Thomason, M.E., Dennis, E., Gotlib, I.H., 2011. Default-mode and task-positive network activity in major depressive disorder: implications for adaptive and maladaptive rumination. Biol. Psychiatry 70, 327–333.

Harrison, B.J., Pujol, J., Ortiz, H., Fornito, A., Pantelis, C., Yucel, M., 2008. Modulation of brain resting-state networks by sad mood induction. PLoS One 3, e1794.

van den Heuvel, M., Mandl, R., Luigjes, J., Hulshoff Pol, H., 2008. Microstructural organization of the cingulum tract and the level of default mode functional connectivity. J. Neurosci. 28, 10844–10851.

Johnson, M.K., Nolen-Hoeksema, S., Mitchell, K.J., Levin, Y., 2009. Medial cortex

activity, self-reflection and depression. Soc. Cogn. Affect. Neurosci. 4, 313–327.
Jung, K.J., 2010. Sensitivity of motion estimation to the anisotropic diffusion of white matter in diffusion MRI., In: Proceedings of the 18th Annual Meeting of the ISMRM., Stockholm, Sweden, p. 4036.
Jung, K.-J., Kohli, N., Yeh, F.-C., Keller, T.A., Zhao, T., 2013. Motion correction in diffusion spectrum imaging using simulated diffusion images at multiple b bands, In: Proceedings of the 21st Annual Meeting of the ISMRM, Salt Lake City, Utah, p. 3192.
Kaiser, R.H., Andrews-Hanna, J.R., Wager, T.D., Pizzagalli, D.A., 2015. Large-Scale Network Dysfunction in Major Depressive Disorder: A Meta-analysis of **Resting**-State Functional Connectivity. JAMA Psychiatry. 72 (6), 603–611. http://dx.doi.org/10.1001/jamapsychiatry.2015.0071.
Kuhn, S., Vanderhasselt, M.A., De Raedt, R., Gallinat, J., 2012. Why ruminators won't stop: the structural and resting state correlates of rumination and its relation to depression. J. Affect. Disord. 141, 352–360.
Leech, R., Kamourieh, S., Beckmann, C.F., Sharp, D.J., 2011. Fractionating the default mode network: distinct contributions of the ventral and dorsal posterior cingulate cortex to cognitive control. J. Neurosci. 31, 3217–3224.
Logothetis, N.K., Wandell, B.A., 2004. Interpreting the BOLD signal. Annu. Rev. Physiol. 66, 735–769.
Lois, G., Wessa, M., 2016. Differential association of default mode network connectivity and rumination in healthy individuals and remitted MDD patients. Soc. Cogn. Affect. Neurosci. 11, 1792–1801.
Lowe, M.J., Koenig, K.A., Beall, E.B., Sakaie, K.A., Stone, L., Bermel, R., Phillips, M.D., 2014. Anatomic connectivity assessed using pathway radial diffusivity is related to functional connectivity in monosynaptic pathways. Brain Connect 4, 558–565.
McGirr, A., Dombrovski, A.Y., Butters, M.A., Clark, L., Szanto, K., 2012. Deterministic learning and attempted suicide among older depressed individuals: cognitive assessment using the Wisconsin Card Sorting Task. J. Psychiatr. Res. 46, 226–232.
Miranda, R., Nolen-Hoeksema, S., 2007. Brooding and reflection: rumination predicts suicidal ideation at 1-year follow-up in a community sample. Behav. Res. Ther. 45, 3088–3095.
Miranda, R., Valderrama, J., Tsypes, A., Gadol, E., Gallagher, M., 2013. Cognitive inflexibility and suicidal ideation: mediating role of brooding and hopelessness. Psychiatry Res. 210, 174–181.
Morcom, A.M., Fletcher, P.C., 2007. Does the brain have a baseline? Why we should be resisting a rest. Neuroimage 37, 1073–1082.
Murphy, K., Birn, R.M., Bandettini, P.A., 2013. Resting-state fMRI confounds and cleanup. Neuroimage 80, 349–359.
Pfefferbaum, A., Chanraud, S., Pitel, A.L., Muller-Oehring, E., Shankaranarayanan, A., Alsop, D.C., Rohlfing, T., Sullivan, E.V., 2011. Cerebral blood flow in posterior cortical nodes of the default mode network decreases with task engagement but remains higher than in most brain regions. Cereb. Cortex 21, 233–244.
Piray, P., den Ouden, H.E., van der Schaaf, M.E., Toni, I., Cools, R., 2015. Dopaminergic modulation of the functional ventrodorsal architecture of the human striatum. Cereb. Cortex..
Reisch, T., Seifritz, E., Esposito, F., Wiest, R., Valach, L., Michel, K., 2010. An fMRI study on mental pain and suicidal behavior. J. Affect. Disord. 126, 321–325.
Serafini, G., Pardini, M., Pompili, M., Girardi, P., Amore, M., 2016. Understanding suicidal behavior: the contribution of recent resting-state fMRI techniques. Front. Psychiatry 7, 69.
Smallwood, J., Fitzgerald, A., Miles, L.K., Phillips, L.H., 2009. Shifting moods, wandering minds: negative moods lead the mind to wander. Emotion 9, 271–276.
Smallwood, J., Karapanagiotidis, T., Ruby, F., Medea, B., de Caso, I., Konishi, M., Wang, H.T., Hallam, G., Margulies, D.S., Jefferies, E., 2016. Representing representation: integration between the temporal lobe and the posterior cingulate influences the content and form of spontaneous thought. PLoS One 11, e0152272.
Smith, S.M., Jenkinson, M., Woolrich, M.W., Beckmann, C.F., Behrens, T.E., Johansen-Berg, H., Bannister, P.R., De Luca, M., Drobnjak, I., Flitney, D.E., Niazy, R.K., Saunders, J., Vickers, J., Zhang, Y., De Stefano, N., Brady, J.M., Matthews, P.M., 2004. Advances in functional and structural MR image analysis and implementation as FSL. Neuroimage 23 (Suppl 1), S208–S219.
Sullivan, P.F., Kessler, R.C., Kendler, K.S., 1998. Latent class analysis of lifetime depressive symptoms in the national comorbidity survey. Am. J. Psychiatry 155, 1398–1406.
Torrey, H.C., 1956. Bloch equations with diffusion terms. Phys. Rev. 104, 563–565.
van Heeringen, K., Bijttebier, S., Desmyter, S., Vervaet, M., Baeken, C., 2014. Is there a neuroanatomical basis of the vulnerability to suicidal behavior? A coordinate-based meta-analysis of structural and functional MRI studies. Front. Hum. Neurosci. 8, 824.
Vanyukov, P.M., Szanto, K., Hallquist, M.N., Siegle, G.J., Reynolds, C.F., 3rd, Forman, S.D., Aizenstein, H.J., Dombrovski, A.Y., 2016. Paralimbic and lateral prefrontal encoding of reward value during intertemporal choice in attempted suicide. Psychol. Med. 46, 381–391.
Varentsova, A., Zhang, S., Arfanakis, K., 2014. Development of a high angular resolution diffusion imaging human brain template. Neuroimage 91, 177–186.
Wechsler, D., 1999. Wechsler Abbreviated Scales of Intelligence (WASI). Psychological Corporation, San Antonio, TX.
Welch, P.D., 1967. The use of Fast Fourier Transform for the estimation of power spectra: A method based on time averaging over short, modified periodograms. IEEE Trans. Audio Electroacoust. AU-15 (2), 70–73. http://dx.doi.org/10.1109/TAU.1967.1161901.
Whitmer, A.J., Banich, M.T., 2007. Inhibition versus switching deficits in different forms of rumination. Psychol. Sci. 18, 546–553.
Whitmer, A.J., Gotlib, I.H., 2012. Switching and backward inhibition in major depressive disorder: the role of rumination. J. Abnorm. Psychol. 121, 570–578.
Whitmer, A.J., Gotlib, I.H., 2013. An attentional scope model of rumination. Psychol. Bull. 139, 1036–1061.
Zhang, S., Chen, J.M., Kuang, L., Cao, J., Zhang, H., Ai, M., Wang, W., Zhang, S.D., Wang, S.Y., Liu, S.J., Fang, W.D, 2016. Association between abnormal default mode network activity and suicidality in depressed adolescents. BMC Psychiatry. 16 (1), 337.

Glossary

SI: suicidal ideators
HC: healthy controls
PCC: Posterior Cingulate Cortex
dACC: Dorsal Anterior Cingulate Cortex
PFC: Prefrontal Cortex
DMN: Default Mode Network
CCN: Cognitive Control Network
SNR: signal to noise ratio
LF BOLD: Low Frequency Blood Oxygenation Level Dependent (signal)
rsfMRI: resting state functional magnetic resonance imaging
GRAPPA: GeneRalized Autocalibrating Partial Parallel Acquisition
DTI: Diffusion Tensor Imaging
FA: fractional anisotropy
RD: radial diffusivity
AD: axial diffusivity
FOV: field of view
P_FWE: family wise error corrected p value.
GLM: general linear model